

EARTHQUAKE ANALYSIS by 3-D MORPHOMETRICS

James L. Farrell, *VIGIL Inc.*

ABSTRACT

Insight into earthquake behavior is obtained by analyzing affine features observed from selected station location histories before and after the Tohoku quake in 2011. Collectively the chosen stations [1] represent a 3-D structure consisting of point masses all tethered to their collective centroid by weightless connecting arms that are not quite rigid. With migration the centroid shifts accordingly while the connecting arms rotate and deform to accommodate as necessary. Irregularities preclude exact characterization for accommodating adjustment patterns, but a daily affine transformation sequence provides a model for interpretation -- with prospects for anticipating earthquakes in the future.

BACKGROUND FROM RELATED FIELDS

The expanded manuscript cited below describes methods adopted from various disciplines (mathematics, mechanics, strength of materials, and anatomy) for this first 3-D affine deformation application to earthquakes. Here only anatomy is discussed in detail, with migrations fit to the five "shape states" involved in 3-D affine deformations, three for shear and two for nonuniform scaling. One way to describe shape states is to note their effects in 2-D, where there is only one for nonuniform scaling (which deforms a square into a rectangle) and one for shear (which deforms a rectangle into a parallelogram). Their usage in anatomy is described next.

Anatomy [5,6]

The topic now to be broached can begin with an example of facial features (e.g., tip of chin, corners of eyes, mouth) exemplifying landmarks identifiable on *any* structures for further study (e.g., diagnosis if deformations correlate with some affliction). When measurements (e.g., from x-ray images) are processed, landmarks – even from a variety of patients (any nationality, any race, all ages, both sexes) – are found to cluster with some degree of consistency. That trait is physiological, not an artifact of processing. When the landmarks are remapped after extracting affine deformations the clusters shrink; theoretically if *only* affine deformations were present, clusters would converge to discrete points. Today's anatomy studies contain thorough descriptions of the entire process with many results and derivations – all in 2-D, thus requiring 3-D extension here. Partial verification of results to be shown is nevertheless offered to the reader; not all results need shape analysis. Some very revealing features arose in earlier portions of the overall procedure – without requiring full pursuit to final determination of 3-D deformations. For this data set, at least, understanding can thus be brought to a significant level with just the *Procrustes* representation, described succinctly as follows:

The structure of K point masses and connecting arms ($K = 11$ in this study) is transformed into principal axes of inertia (next subsection) and the origin is translated to the centroid. Division by root sum square of all coordinates then produces an array containing $3K$ dimensionless positive and negative numbers whose sum of squares is unity.

With normalization of all magnitudes an orthogonal matrix, computed for each separate day of the sequence, minimizes that day's sum of squares of rotated landmark changes from the first ("Day #I"). It is formed as a product $\mathbf{M}_V \mathbf{M}_U^T$ of outer factors from svd with \mathbf{U} and \mathbf{V} , $3 \times K$ matrices produced by the Procrustes operations just defined, acting on data from Day #I and each subsequent day, respectively.

After forming all Procrustes coordinate matrices and storing columns of \mathbf{U} into vector \mathbf{U} , affine transformation provides an array \mathbf{u} of small adjustments for each day's fitted array \mathbf{V} , nominally characterized as $\mathbf{U} + \mathbf{u}$ – with one departure from anatomy applications: here there is no average mesh; Day #I's coordinate set serves as the comparison reference throughout. Also the coordinate adjustments, shape states, and rotations from svd here are not merely small; they are minuscule – of order $1.e-8$. Still the need for precision calls for rigorous computations; over a span of 1000 km, 0.01μ radian rotations generate cm displacements. .

PROCEDURE

A synopsis of steps summarizes the preceding descriptions:

- select an ensemble of station histories to be analyzed
- acquire data in most reliable and accurate form
- assemble coordinate data into arrays to prepare operations
- use each separate day's landmark set centroid as origin
- form the inertia matrix of the first day's landmark set
- diagonalize the inertia matrix for principal axis resolution
- form a direction cosine matrix from the eigenvectors
- shrink each day's centered landmark coordinate sum of squares to unity
- transform each day's landmark data set through the 3×3 orthogonal matrix
- rotate again per svd from each day's data vs Day #I
- compute estimates for each day's five shape states
- apply shape states to the reference (Day #I) data
- backtrace steps to reconstruct input data; evaluate the fit based on residuals, interpret and document comparisons.

QUANTITATIVE RESULTS

Permanent pre-to-post-quake change was unsurprising – but unexpected behavior serendipitously arose while validating the small-angle rotations. The orthogonal matrix formed from svd outer factors previously described provided the minimization promised. Verifying that produced Figure 1:

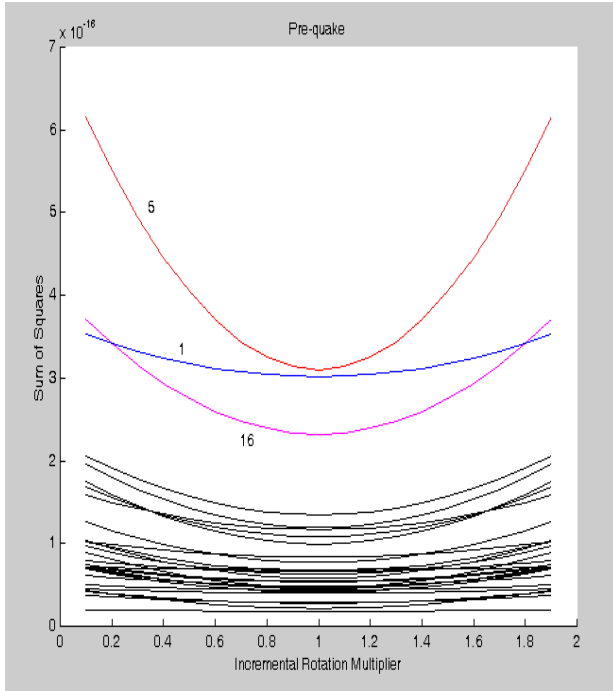


Figure 1: Rotation sensitivity before quake

Figure 1 was generated as follows: Separately in sequence, centroids of each day's K landmark appendages colocate with that of Day #I. Migration nonuniformity precludes coincidence of point mass extremities but the sum of squared separation distances is minimized by the orthogonal matrix from svd. Multiplying the angle through a span of values (from too little to too much rotation) always made the closest combination for a multiplier of unity. The sum of squares grows gradually as the quake draws near *except* for the days showing abnormal departures in Fig 1. One quake cannot establish a rule but wider investigation is warranted.

Before attention is shifted to shape it is reiterated that behavior of this data set is not guaranteed to hold in general. Other attributes could arise from chosen landmark sets with dissimilar layout geometries (or from an alternative choice of shape states for this data set – 2 expansion / contraction states cover 3 directions). No generalization is attempted here; data from other quakes could show different behavior.

The volume of data (in three directions from eleven landmarks over a period of weeks) necessitated a way to compact the results for this affine model. That effort, applied to RSS values (3-D x, y, z), produced Figure 2.

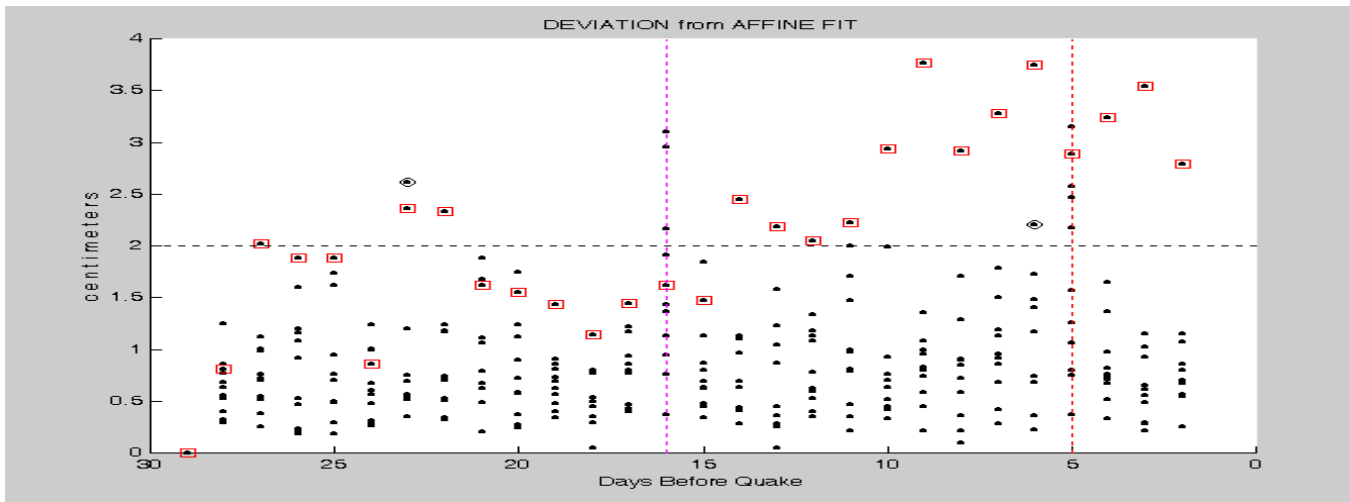


Figure 2: Complete set of RSS residuals (near-epicenter values enclosed within a square), approx. 2 cm dispersion range

Most residuals in Figure 2 (shown with a dot •) fall very near or below the dashed horizontal line at 2 cm. Exceptions are

- values obtained at 16 and 5 days pre-quake (the main "early warning" days, light dashed vertical lines)
- landmark #5 (closest to the epicenter), whose residuals are enclosed within a square
- two others (shown encircled) at about 2.2 and 2.6 cm.

All residuals are below 4 cm., almost 98% are below 3, and over 91% are below 2. All but two values significantly above 2 cm are either from the station nearest epicenter or from one of the key early warning days.

The above plot of this full set was preceded by partial glimpses. With 3-D RSS migration reaching a maximum of almost 15 cm amidst dispersions of a few cm, these results are consistent with performance expected from minimum variance estimation. By analogy with a straight line or low order curve fitted to scattered empirical data, a least squares fit here captures the larger migrations while accepting residuals commensurate with the dispersion in the data. The fitted model will not *adhere* to the points; model credence rests on acceptance of 2-cm residuals as a reasonable price to pay for a means of characterization.

Immediately a caveat might be raised: Shouldn't that be changed – contingent on acceptance of 4-cm residuals ? Actually no; aside from the two circled points in Figure 2 (beyond 2 cm by modest amounts), the "problem" of larger residuals is in reality the *opposite* of a problem. They offer valuable revelations, in time (premonitions at 16 and 5 days pre-quake) and spatially – most of them correspond to the landmark closest to epicenter ! As with other facets of this investigation, no generalization will be attempted – but other quakes should be examined for these traits.

DATA FOR VERIFICATION

The extended manuscript included data enabling duplication of results, by methods applicable also to observations from other quakes. Coordinates at Day #I and at 5 days pre-quake allowed validating the top curve of Figure 1, and additional data tabulated accuracy evaluation for the affine fit, as a product of a $3K \times 5$ matrix and a 5×1 shape state. Reconstruction showed small residuals with relatively large migrations. The fit provides awareness of large landmark excursions while "muddling and muddling through" the smaller, while giving advance clues in time and location.

CONCLUSIONS AND RECOMMENDATIONS

Results justify advocacy for accumulating a data base, by applying morphometrics to several known quake histories. That effort could employ variations in, and extensions of, methods used here. Further applications (with suitable modification): *tsunami prediction* and *aging infrastructure*.

ACKNOWLEDGMENT

Prof. Frank van Graas and Ryan Kollar of Ohio University provided all landmark data for this investigation. Without their diligent acquisition *and validation* of the data, none of the results presented here could have been generated.

HISTORICAL NOTE

Physiological studies of affine deformations in current practice ironically lack a crucial feature; they concentrate heavily on two-dimensional representations. While full affine representation is very old, its inversion (i.e., optimal estimation of shape states from a given overdetermined coordinate set) has heretofore been limited to 2-D. Immediately then, extension was required for adaptation. The fundamentals still remain applicable, however, as indicated by plots presented in this paper.

REFERENCES

- [1] F. van Graas and R. Kollar, "Processing of GPS Station Data for Prediction Algorithm Analysis of the 2011 Tohoku Earthquake," ION Pacific PNT 2013.
- [2] J.L. Farrell, Integrated Aircraft Navigation, Academic Press, 1976 (now in paperback; – <http://jameslfarrell.com/published-books-gnss-aided-navigation-and-tracking>)
- [3] J.L. Farrell, GNSS Aided Navigation and Tracking, Amer. Literary Press, 2007 (<http://jameslfarrell.com/wp-content/uploads/2012/03/GPSINS.pdf>).
- [4] D.F. Rogers and J.A. Adams, Mathematical Elements for Computer Graphics (2 ed), McGraw-Hill, 1990.
- [5] M. Zelditch et. al., Geometric morphometrics for biologists: a primer, Academic Press, 2004, ISBN 0-12-77846-08, pages 137-142.
- [6] F. Bookstein, "Shape and the Information in Medical Images: A Decade of the Morphometric Synthesis," Computer Vision and Image Understanding, v66 n2, May 1997, pp. 97-118.